Supporting Information for

A Selenium-Based NIR-II Photosensitizer for a High Effective and Safe Phototherapy Plan

Xiangqian Zhang,[+a] Chonglu Li,[+c] Xiaofang Guan,[+d] Yu Chen,[a] Qingqing Zhou,[a] Huili Feng,[a] Yun Deng,[e] Cheng Fu,[e] Ganzhen Deng,[a] Junrong Li,*[c] Shuang Liu*[b]*

a. State Key Laboratory of Agricultural Microbiology, College of Veterinary Medicine, Huazhong Agricultural University, Wuhan 430070, China

b. School of Materials Science and Engineering, Wuhan University of Technology, 122 Luoshi Road, Wuhan 430070, China

c. National Key Laboratory of Green Pesticides, College of Chemistry, Central China Normal University, Wuhan 430079, China

d. Hubei Province Key Laboratory of Occupational Hazard Identification and Control, Wuhan University of Science and Technology, Wuhan 430081, China

e. Key Laboratory of Optoelectronic Chemical Materials and Devices of Ministry of Education, Jianghan University, Wuhan 430056, China

* Corresponding authors: Email: ganzhendeng@sohu.com (G.D.); junrong.li@ccnu.edu.cn (J.L); shuangliu@whut.edu.cn (S.L.)

+ These authors contributed equally

Table of Contents

General materials and instruments

Materials. Dulbecco's modified eagle medium (DMEM), and fetal bovine serum (FBS) were purchased from Gibco (Australia). 3-(4,5-dimethylthiazol-2-yl)-2, 5-diphenyltetrazolium bromide (MTT) were obtained by BioFrox (Guangzhou, China). Trypsin-EDTA solution were purchased from Beyotime Biotechnology (Shanghai, China). 2',7'-dichlorofluorescein diacetate (H2-DCFH), and 1,3-diphenylisobenzofuran (DPBF) purchased from Sigma-Aldrich (Poole, UK). Mito-Tracker Red CMXRos, propidium iodide (PI), were obtained from Solarbio (Beijing, China). DSPE-PEG5000 was purchased from Avanti Polar Lipids.

Instruments. Nuclear magnetic resonance (NMR) spectra were obtained using a Varian Inova 400/600 MHz NMR spectrometer. Electro Spray Ionization-Mass Spectroscopy (ESI-MS) spectra were recorded on a Micromass Quattro II triple-quadrupole mass spectrometer or Synapt G2-Si mass spectrometer using electrospray ionization with a MassLynx operating system (Waters, USA). Absorption spectra were measured on a UV-vis-NIR spectrophotometer (Shimadzu UV-3600, Japan). Fluorescence spectra were measured on a Fluorolog-3 spectrofluorometer (Horiba Jobin Yvon, France) and the fluorescence emitting within the NIR-II region were measured by a Cary Eclipse fluorophotometer. The laser of 808-nm wavelength was purchased from Beijing Hi-Tech Optoelectronic (China). The infrared (IR) photos were captured by IR camera (Fluke, Ti400, USA). *In vivo* NIR-II imaging was carried on Suzhou NIR-Optics imaging system. Flow cytometry was performed on Beckman (USA). Hydrodynamic diameter and zeta potential were tested by Malvern Zetasizer Nano ZS. Transmission electron microscopy (TEM) images were captured on Hitachi HT-7700 (Japan).

Experimental section

Preparation of Se-IR1100 NPs. The mixture of **Se-IR1100** solution (1 mg in 1 mL acetonitrile) and DSPE-PEG5000 solution (9 mg in 9 mL PBS) were stirred overnight. After the removal of acetonitrile by using nitrogen gas flow, the residual water was removed by centrifugation (3000 rpm, 20 min) with a 50 kDa centrifugal filter to provide the **Se-IR1100** NPs.

***In Vitro* Photo-stability Test. Se-IR1100** NPs (20 μM) or ICG (20 μM) aqueous solution was continuously irradiated under 808 nm laser at 0.03 W cm^{-2} for 30 min. The absorbance at 845 or 780 nm was measured every 5 min by using a SpectraMax M5 microplate reader.

***In Vitro* Photothermal Test. Se-IR1100** NPs (0, 10, 20, 40 μM) and ICG (40 μM) aqueous solution was continuously irradiated under 808 nm laser (1 W cm^{-2}, 5 min) and the temperature change was monitored by using a photothermal camera (Fluke, Ti400, USA).Six cycles of on/off NIR laser irradiation on the **Se-IR1100** NPs (40μM) or ICG (40 μM) were performed (808 nm, 1.0 W cm^{-2}, laser on for 5 min and laser off for 5 min). The photothermal conversion efficiency (PCE) of **Se-IR1100** NPs and ICG was calculated according to the published method [1], in which T_{max} (or T_{sur}) is the equilibrium temperature (or ambient temperature), I was the incident laser power (I = 1 W cm^{-2}), A808 is the absorbance at 808 nm, and τ_s is the system time constant of the sample.

$$\mathrm{PCE} = \frac{\mathrm{hs}\,(\mathrm{T_{max}} - \mathrm{T_{sur}}) - Q_0}{\mathrm{I}\,(1 - 10^{-\mathrm{A808}})}$$

$$\mathrm{h_s} = \frac{\Sigma_i\, \mathrm{m}_i\, \mathrm{C}_{p,i}}{\tau_\mathrm{s}}$$

$$\tau_\mathrm{s} = \frac{t}{-ln\theta} = \frac{t}{-\ln\left(\frac{(\mathrm{T} - \mathrm{T_{sur}})}{(\mathrm{T_{max}} - \mathrm{T_{sur}})}\right)}$$

Detection of ROS *in vitro*. The ROS generation efficacy of **Se-IR1100** NPs was estimated by commonly-used ROS indicator DCFH-DA [2]. 0.5 mL of a 1 mM DCFH-DA solution (in DMSO) was mixed with 2 mL of a 10 mM NaOH solution (in water) to deacetylate into DCFH. The 1.6 μL activated DCFH (50 μM) was added into 400 μL

Se-IR1100 NPs (20 μM in PBS) or PBS only, and then the mixed solution was exposed to laser irradiation (808 nm, 1 W cm^{-2}, 5 min). The DCF fluorescence spectra (Ex/Em=488/525 nm) were recorded. The HPF and DHR123 test ·OH, and $\cdot O_2^-$ at the same conditions. The mixture of 16 μL DPBF (1 mg mL^{-1} in ethanol) and 400 μL **Se-IR1100** NPs solution (20 μM) was irradiation by 808 nm laser (1 W cm^{-2}, 5min) to detect the production of $^1O_2$, which was measured by the decline of UV-Vis absorption at 416 nm. The ABDA was also utilized as an indicator to survey the $^1O_2$ generation ability and the absorption at 378 nm. In addition, the capturing agent, 2, 2, 6, 6-tetramethylpiperidine (TEMP) and 5,5-Dimethyl-1-pyrroline N-oxide (DMPO) was used to detect the generation of $^1O_2$ and •OH via the ESR spectrometer, respectively. 100 μL **Se-IR1100** NPs was exposed to 808 nm laser irradiation for 5 min in the presence of TEMP (2.5 μL). The $^1O_2$ generation signal was detected via the ESR spectrometer. For the detection of •OH radicals, the TEMP was replaced by 5 μL DMPO.

Singlet Oxygen Quantum Yield. To measure the singlet oxygen quantum yield (Φ_Δ) of **Se-IR1100** NPs, we use DPBF as an indicator and ICG as a reference compound with a known ΦΔ value of 0.14. The solutions of **Se-IR1100**NPs (20 μM) and ICG (20 μM) containing 16 μL DPBF (1 mg mL^{-1} in ethanol) were irradiated at 808 nm (1 W cm^{-2}) for 5min, respectively. The absorbance of DPBF at 416 nm was measured. Φ_Δ was calculated using the equation of $\Phi_\Delta = (\Phi_\Delta{}^{ICG} \cdot W \cdot I^{ICG}) / (W^{ICG} \cdot I)$ [3].

The ROS penetration depths and the FL penetration depths measurement of Se-IR1100 NPs. 1% intralipid (a mixture of 5 mL of 20% intralipid with 100 mL of water) was used to mimic biological tissue to detect **Se-IR1100** NPs (20 μM) producing ROS in deep tissues under 808 nm laser irradiation. The depth of the biological tissue was calculated from the area of the dish. To investigate the FL of **Se-IR1100** NPs and ICG in tissue penetration depth, glass capillary tubes filled with **Se-IR1100** NPs (20 μM) or ICG (200 μM) were placed at the bottom of a cylindrical dish filled with varied volumes of intralipid to simulate the wavelength dependency of light scattering in biological tissues. The fluorescence images were then obtained by using 808 nm laser illumination

for **Se-IR1100** NPs, and 780 nm laser illumination for ICG. Images were analyzed by Image J software.

Cell apoptosis and fluorescence detection by flow cytometry. To investigate the apoptotic effects of **Se-IR1100** NPs on HeLa cells, the cells in various treatment groups were processed according to the protocol provided with the apoptosis kit (Annexin V-FITC/PI) and performed on flow cytometry (Ex/Em = 488/525 nm, Ex/Em = 535/615 nm).

***In vivo* and *ex vivo* NIR-II fluorescent imaging.** The tumor bearing nude mice was administered **Se-IR1100** NPs intravenously (200 μM, 0.2 mL) and the fluorescence images were captured using NIR-II FLI system at various time points (0 h to 48 h). The imaging data were analyzed using ImageJ software.

Cell viability assay. HeLa or 4T1 cells were seeded in 96-well plates at 1×10^4 cells/well for 24 hours followed by culture medium removal and subsequently addition of culture medium containing **Se-IR1100** NPs at different concentrations. After incubation of 12 h, the cell viability was evaluated by MTT assay according to the manufacturer's protocol after the cells treated with or without light illumination. For photodynamic therapy, the cells were separately placed in a 96-well plate on ice with 808 nm irradiation (1 W cm^{-2}, 5 min).

Intracellular ROS measurement. HeLa cells were incubated with **Se-IR1100** NPs (20 μM, 400 μL) for 12 h. Afterward, a DCFH-DA fluorescent probe (20 μM, 1.6 μL) was added to the cells and allowed to incubate for 30 min in the dark. The cells were then exposed to laser irradiation (808 nm, 1 W cm^{-2}, 5 min). After irradiation, the cells were washed twice with PBS and *in vitro* FLI was performed by a LeicaSP8 confocal laser scanning microscope (CLSM) (Ex/Em = 488/525 nm).

Hemolysis assay. Fresh blood from healthy nude mice was obtained in heparinized tubes from mice, and then washed by PBS (3000 rpm, 10 min) three time. **Se-IR1100** NPs were prepared with varying concentrations (ranging from 50 to 400 μM) in a

constant volume of 0.8 mL PBS, to which 0.2 mL of the RBC solution was added. The mixture was then incubated in a shaking water bath at 37°C for 1 hour. Then all suspensions were centrifugation at 3000 rpm for 10 min. After that, the supernatant absorbance at 540 nm was recorded. The hemolysis rate was calculated by using the following equation.

$$\text{Hemolysis Rate (\%)} = (OD_{sample} - OD_{saline}) / (OD_{water} - OD_{saline}) \times 100\%$$

Xenograft tumor model. 4T1 cells (1×10^6 in 50 μL PBS) were injected subcutaneously into the right thigh of female nude mice (Suzhou Belda Bio-Pharmaceutical Co.). When tumor volume reached to 50 ~ 100 mm^3, the nude mice bearing xenograft 4T1 tumors were subjected to further experiments.

***In vivo* phototherapy.** 4T1-tumor-bearing mice (18 - 20 g, 5 weeks old) were randomly assigned to 4 groups (n = 4), including 1) control group (PBS), 2) **Se-IR1100** NPs group (0.2 mL, 200 μM), 3) only Laser group (PBS), 4) Laser + **Se-IR1100** NPs group. Meanwhile, 4T1 tumor-bearing mice of the (3) and (4) group received laser irradiation (808nm, 1 W cm^{-2}, 10 min) at 48 hours after injection. Tumor volume was assessed by applying the following formula: Volume = (tumor length) × $(\text{tumor width})^2/2$.

Statistical analysis. Statistical differences were compared by unpaired Student's *t*-tests analyzing used GraphPad Prism 9 software. * $p<0.05$, ** $p<0.01$, *** $p<0.001$, **** $p<0.0001$.

Synthetic procedures and characterization:

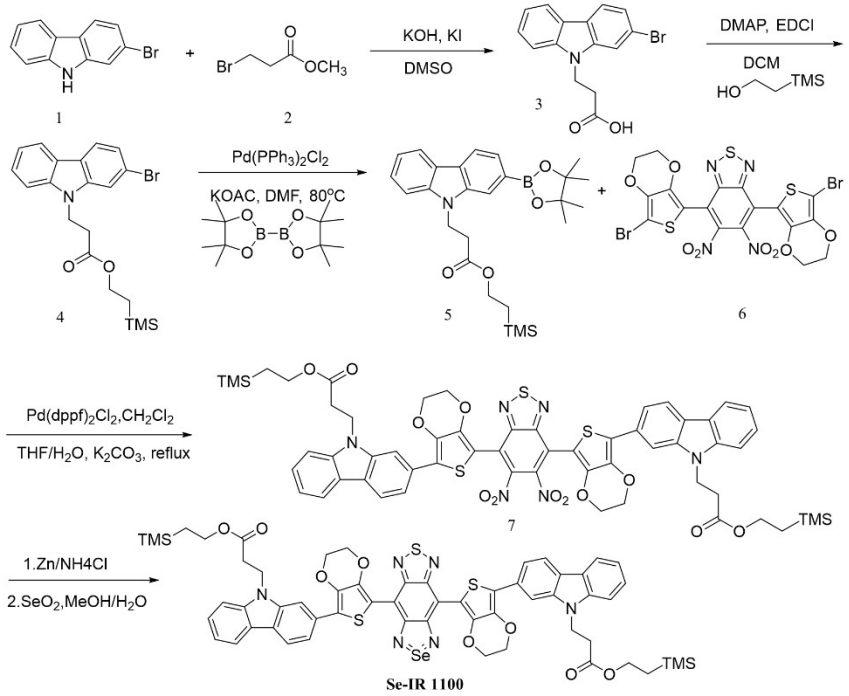

Scheme 1. The Synthesis of **Se-IR1100**.

*Synthesis of Compound **3***:

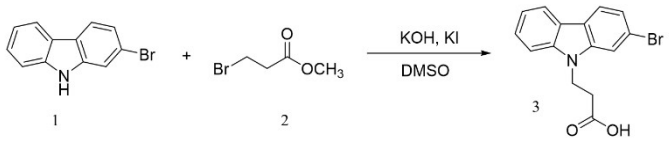

2-bromocarbazole (1.50 g, 6.10 mmol) and potassium iodide (101.3 mg, 0.61 mmol) were dissolved in dimethyl sulfoxide (20 mL) under argon protection. Methyl 3-bromopropionate (2.00 mL, 18.3 mmol, 3.06 g) was added to the reaction mixture. Potassium hydroxide (1.71 g, 30.5 mmol) was then added to the solution in 10 parts. The reaction solution was heated to 95°C for 24 h and quenched with water. The mixture was acidified to pH = 5 with 2 M hydrochloric acid aqueous solution, dried with anhydrous magnesium sulfate after extraction with ethyl acetate, and concentrated to obtain compound 2-3 (1.67 g, 88 %) as a white solid, and the crude product was directly used for the next reaction without purification. ^{1}H NMR (400 MHz, DMSO-d6) δ 8.14 (d, J = 7.6 Hz, 1H), 8.08 (d, J = 8.2 Hz, 1H), 7.90 (s, 1H), 7.62 (d, J = 8.2 Hz, 1H), 7.46

(t, *J* = 7.6 Hz, 1H), 7.32 (d, *J* = 8.2 Hz, 1H), 7.22 (t, *J* = 7.4 Hz, 1H), 4.59 (t, *J* = 6.8 Hz, 2H), 2.67 (t, *J* = 6.8 Hz, 2H).^{13}C NMR (101 MHz, DMSO) δ 173.46, 141.17, 140.40, 126.70, 122.54, 121.86, 121.77, 120.85, 119.86, 119.05, 112.85,110.15, 34.62.

*Synthesis of Compound **4***:

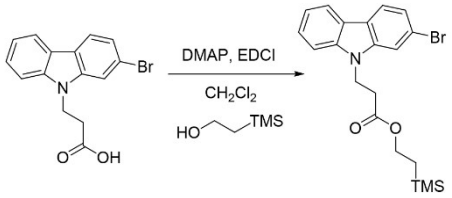

3 4

Compounds **3** (1.67 g, 5.23 mmol) were dissolved in dichloromethane (24 mL) under argon protection. 2-trimethylsilylethanol (1.2 mL, 8.37 mmol, 989.52 g) was added after 30 minutes of reaction with 1-(3-dimethylaminopropyl)-3-ethylcarbodiimide hydrochloride (EDCI) (1.60 g, 8.37 mmol) and 4-dimethylaminopyridine (DMAP) (64.2 mg, 0.523 mmol). The reaction mixture was stirred for 12 h at room temperature. Diluted with dichloromethane (300 mL), the organic layer was extracted with saturated ammonium chloride solution (100 mL), water (4×100 mL), saturated saline (100 mL) and dried by anhydrous magnesium sulfate. After the organic layer was concentrated, it was purified by silica gel column (petroleum ether: ethyl acetate = 32:1, v/v) to obtain yellow oily liquid compound 4 (1.52 g, yield 69.4 %). ^{1}H NMR (400 MHz, $CDCl_3$) δ 7.99 (dd, *J* = 7.6, 3.2 Hz, 2H), 7.86 (s, 1H), 7.67 (d, *J* = 7.8 Hz, 1H), 7.39-7.34 (m, 2H), 7.14 – 7.09 (m, 1H), 4.56 (t, *J* = 7.2 Hz, 2H), 4.04-4.00 (m, 2H), 2.72-2.70 (m, 2H), 1.33 (s, 12H), 0.78-0.72 (m, 2H), 0.07 (s,9H).^{13}C NMR (101 MHz, $CDCl_3$) δ 171.25, 140.44, 139.41, 126.32, 125.53, 122.74, 120.66, 119.53, 119.11, 114.90, 108.82, 77.79, 77.47, 77.15, 62.83, 38.60, 33.67, 24.92, 17.02, 1.59.

*Synthesis of Compound **5***:

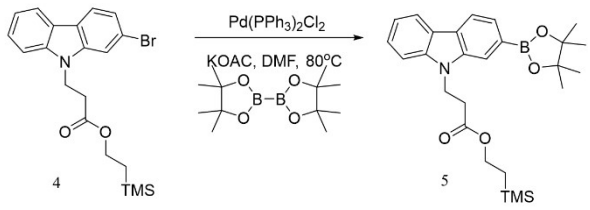

Compounds **4** (1.52 g, 3.62 mmol), biquinolborrate (1.65 g, 6.52 mmol), potassium acetate (853.72 g, 8.70 mmol) and bis(triphenylphosphine) palladium (II) dichloromethane complex (260.3 mg, 0.362 mmol) were dissolved in N, N-dimethylformamide (20 mL) for anhydrous oxygen-free argon protection. The reaction solution was then reacted at 80 °C for 12h. After the reaction is complete, ethyl acetate (60 mL) is added and solids are removed by filtration. Dilute the solution with water (120 mL) and extract the organic phase with methylene chloride (3 × 60 mL). Extracted with water (4 × 60 mL), saturated saline (150 mL) and dried with anhydrous magnesium sulfate. After organic phase concentration, it was purified by silica gel column (petroleum ether: ethyl acetate = 16:1, v/v) to obtain colorless oil liquid compound 5 (1.46 g, yield 87.4%). ^{1}H NMR (400 MHz, $CDCl_3$) δ 7.99 (dd, *J* = 7.6, 3.2 Hz, 2H), 7.86 (s, 1H), 7.67 (d, *J* = 7.8 Hz, 1H), 7.39-7.34 (m, 2H), 7.14-7.09 (m, 1H), 4.56 (t, *J* = 7.2 Hz, 2H), 4.04-4.00 (m, 2H), 2.72-2.70 (m, 2H), 1.33 (s, 12H), 0.78-0.72 (m, 2H), 0.07 (s,9H).^{13}C NMR (101 MHz, $CDCl_3$) δ 171.25, 140.44, 139.41, 126.32, 125.53, 122.74, 120.66, 119.53, 119.11, 114.90, 108.82, 77.79, 77.47, 77.15, 62.83, 38.60, 33.67, 24.92, 17.02, 1.59.

Synthesis of Compound 7:

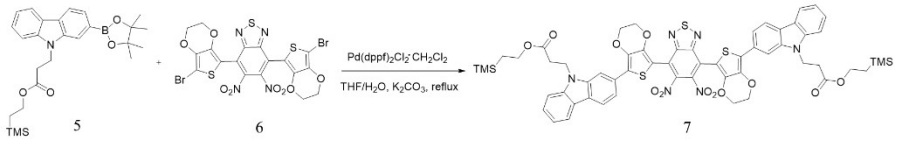

Argon was introduced into tetrahydrofuran (12 mL) solutions for compounds **5** (447.2 mg, 0.96 mmol) and 6 (288.6 mg, 0.43 mmol) for 5 min. Under the protection of argon, a solution of potassium carbonate (165.7 mg, 1.2 mmol) water (3.0 mL) and

1, 1, - bis (diphenylphospho) palladium (II) palladium dichloride dichloride (20.42 mg, 0.024 mmol) was added to the above reaction mixture. The mixture reacts in an oil bath at 75 °C for 8 h. After cooling to room temperature, the solvent is removed by vacuum. The residue is extracted with water and ethyl acetate and dried with anhydrous magnesium sulfate. The crude product was purified by silica gel column (petroleum ether: ethyl acetate = 10:1, v/v) to obtain blue solid compound 6 (210 mg, yield 41.2%). ^{1}H NMR (400 MHz, $CDCl_3$) δ 8.12 (t, *J* = 6.8 Hz, 4H), 7.94 (s, 2H), 7.80 (d, *J* = 8.0 Hz, 2H), 7.50 (d, *J* = 3.6 Hz, 6H), 4.73 (s, 4H), 4.57 (d, *J* = 2.8 Hz, 4H), 4.43 (d, *J* = 2.4 Hz, 4H), 4.20-4.13 (m, 4H), 2.91 (t, *J* = 7.2 Hz, 4H), 0.91 (d, *J* = 7.6 Hz, 4H), 0.01 (s, 18H). ^{13}C NMR (101 MHz, $CDCl_3$) δ 171.60, 152.64, 143.20, 142.86, 140.73, 140.22, 137.44, 129.66, 126.14, 125.31, 122.87, 120.58, 119.57, 118.35, 108.83, 106.76, 102.81, 64.59, 63.28, 38.83, 33.70, 17.17, 0.00.

Synthesis of Compound ***Se-IR1100***

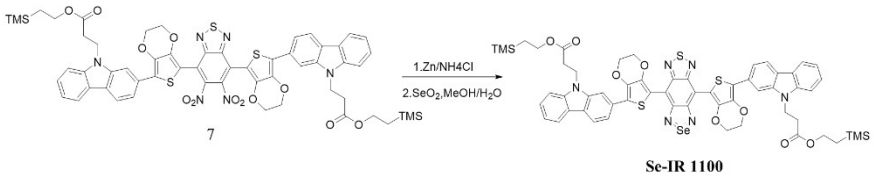

7 **Se-IR 1100**

(1) Zinc powder (132.6 mg, 2.04 mmol) and ammonium chloride (57.21 mg, 1.02 mmol) were added to a mixture solution of solubilized compounds 2-7 (21.0 mg, 0.017 mmol), dichloromethane (4 mL), and 90 % methanol (4 mL) in a 25 mL round-bottom flask. Allow the reaction mixture to react for 3 h at room temperature. The reaction solution was filtered through a diatomaceous earth pad, then dried by anhydrous magnesium sulfate and evaporated under vacuum. The crude product does not need to be purified and is used directly for the next step of the reaction.

(2) Add water (1 mL) and selenium dioxide (4.15 mg, 0.037 mol) to the yellow-green methanol (2 mL) solution. The solution was heating in an oil bath at 60°C for 3 h. The reaction solution was cooled to room temperature, extracted with water and ethyl

acetate (3 × 10 mL), dried by anhydrous magnesium sulfate and vacuumed. The residue was purified by column chromatography on silica gel and eluted with petroleum ether and ethyl acetate (petroleum ether/ethyl acetate = 2/1, v/v) to obtain the product **Se-IR1100** as green solid (8.0 mg, yield 40 %). ^{1}H NMR (400 MHz, $CDCl_3$) δ 8.11 (t, *J* = 6.8 Hz, 4H), 7.96-7.75 (m, 4H), 7.49 (d, *J* = 2.6 Hz, 4H), 7.28-7.23 (m, 2H), 4.73 (t, *J* = 7.2 Hz, 4H), 4.57 (s, 4H), 4.42 (s, 4H), 4.20-4.13 (m, 4H), 2.91 (t, *J* = 7.2 Hz, 4H), 0.90 (s, 4H), 0.00 (s, 18H). ^{13}C NMR (101 MHz, $CDCl_3$) δ 173.09, 153.83, 153.53, 142.33, 141.90, 133.72, 132.35, 130.14, 127.96, 125.66, 125.24, 124.30, 122.54, 122.15, 121.98, 121.28, 119.60, 110.43, 107.78, 64.92, 40.42, 35.32, 18.73, 0.00. MS (MALDI-TOF) m/z: calcd. for: $C_{58}H_{56}N_6O_8S_3SeSi_2^+$: calcd. 1196.20, found: 1196.2074.

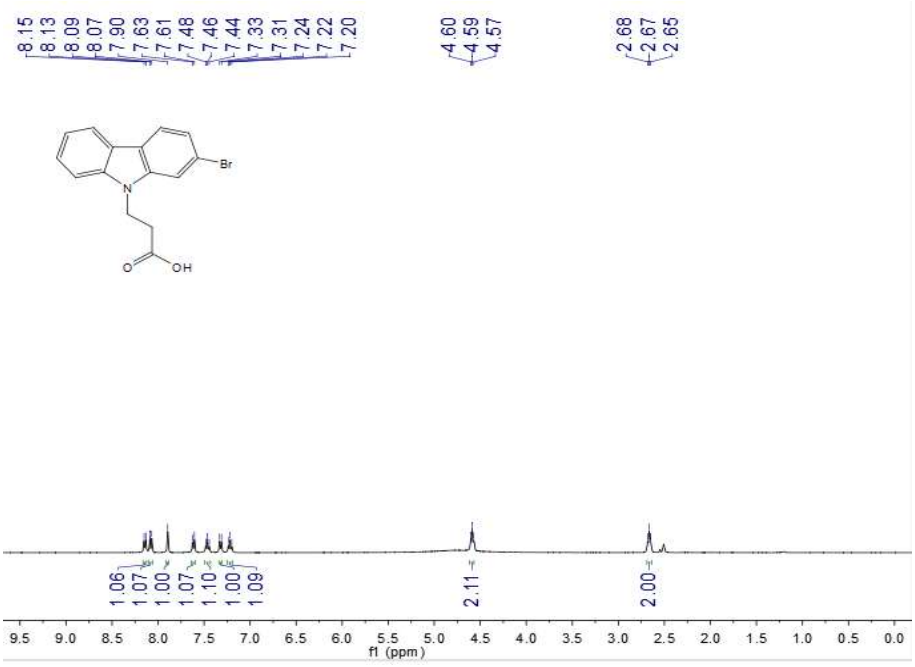

Figure S1. ^{1}H NMR spectrum (400 MHz, $CDCl_3$, 298 K) of **3**.

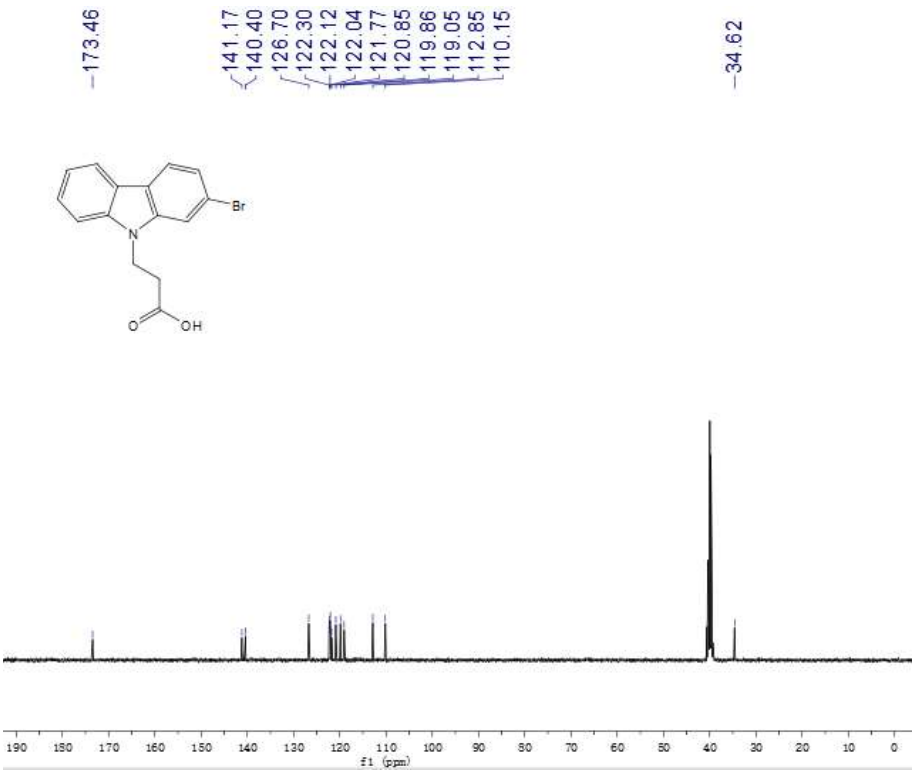

Figure S2. ^{13}C NMR spectrum (400 MHz, CDCl3, 298 K) of **3**.

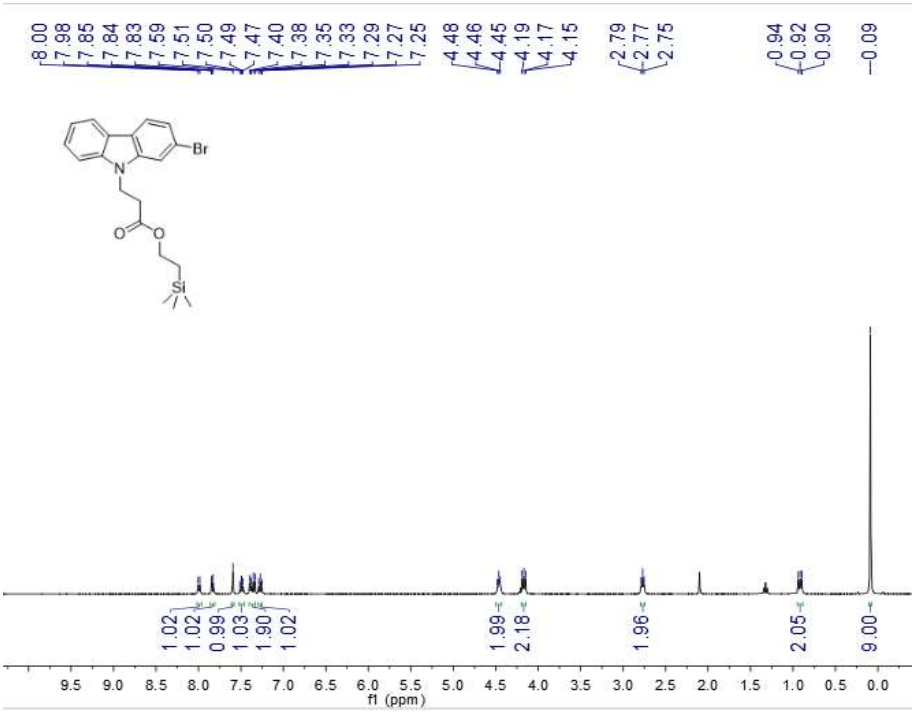

Figure S3. ^{1}H NMR spectrum (400 MHz, $CDCl_3$, 298 K) of **4**.

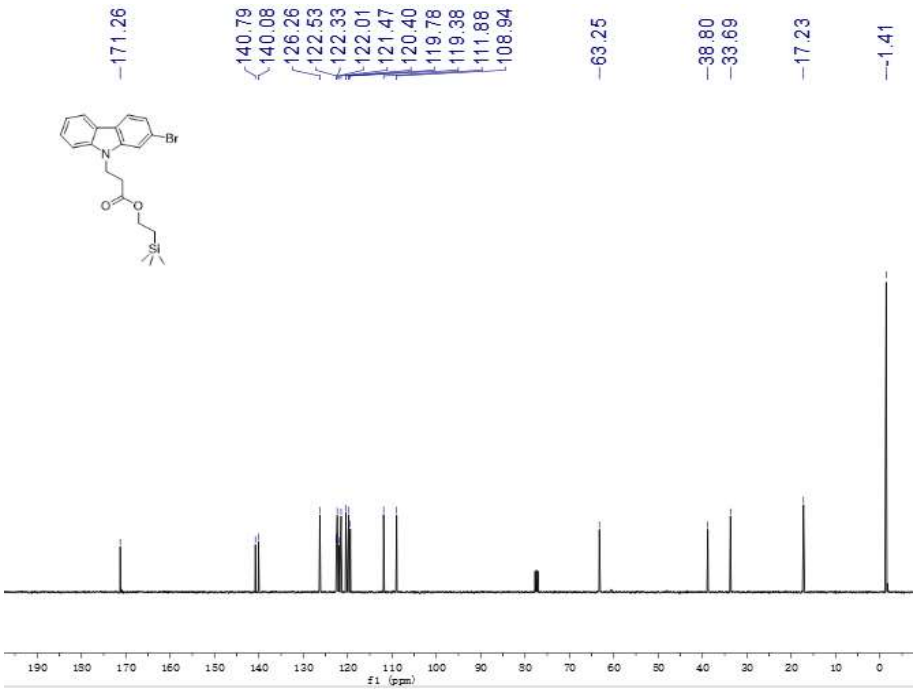

Figure S4. ^{13}C NMR spectrum (400 MHz, CDCl3, 298 K) of **4**.

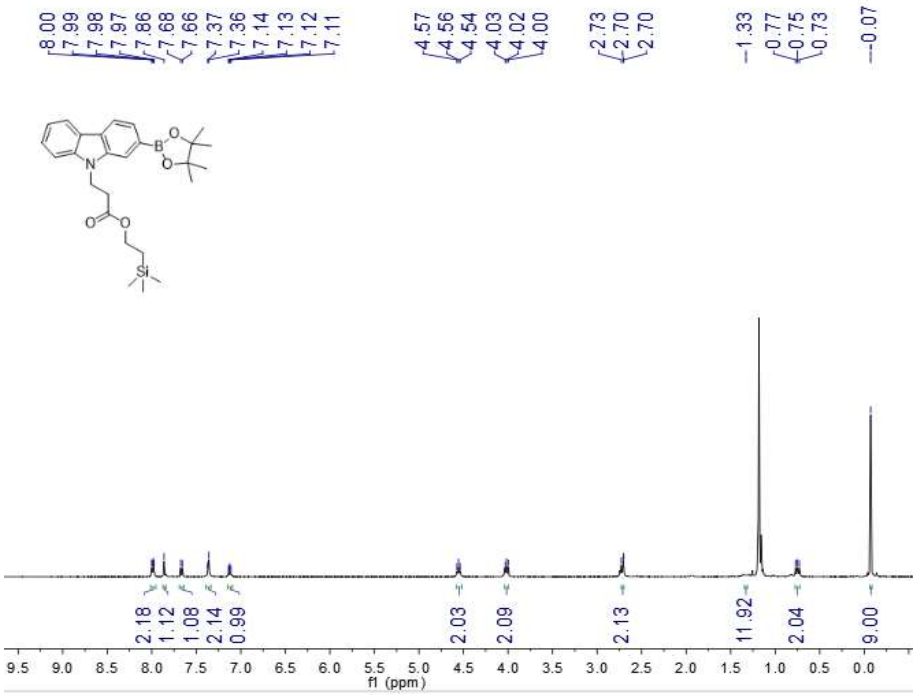

Figure S5. ^{1}H NMR spectrum (400 MHz, $CDCl_3$, 298 K) of **5**.

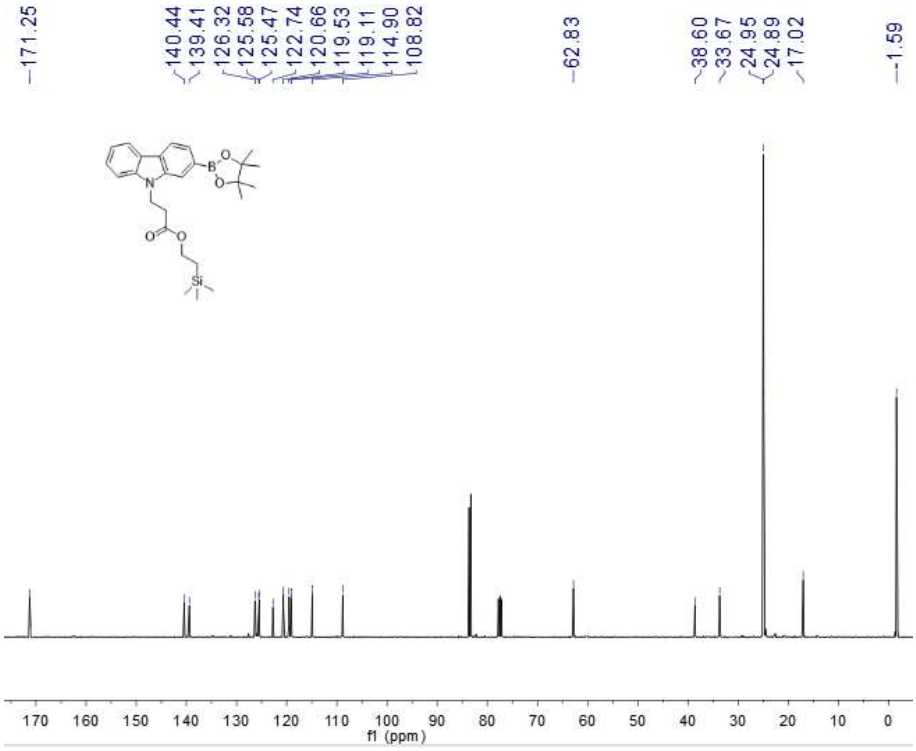

Figure S6. ^{13}C NMR spectrum (400 MHz, CDCl3, 298 K) of **5**.

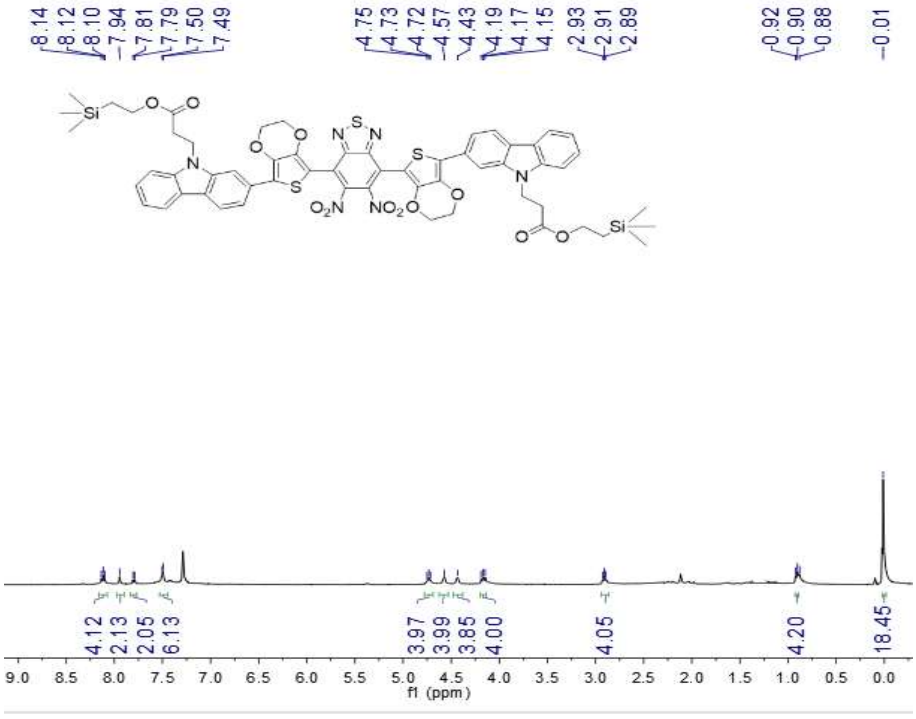

Figure S7. ^{1}H NMR spectrum (400 MHz, $CDCl_3$, 298 K) of **7**.

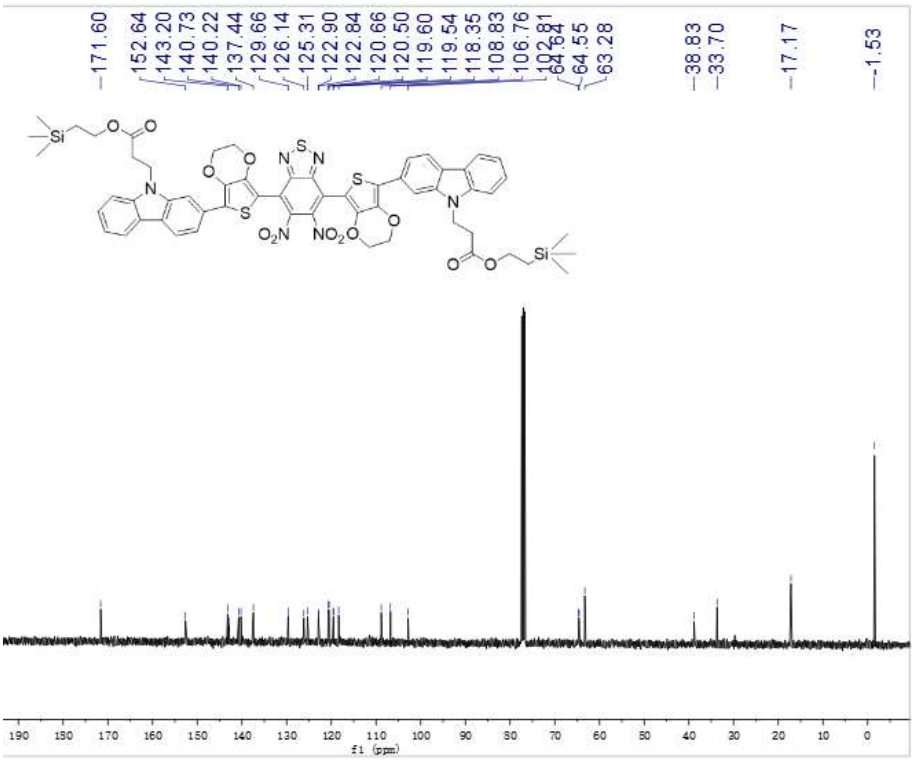

Figure S8. ^{13}C NMR spectrum (400 MHz, CDCl3, 298 K) of **7**.

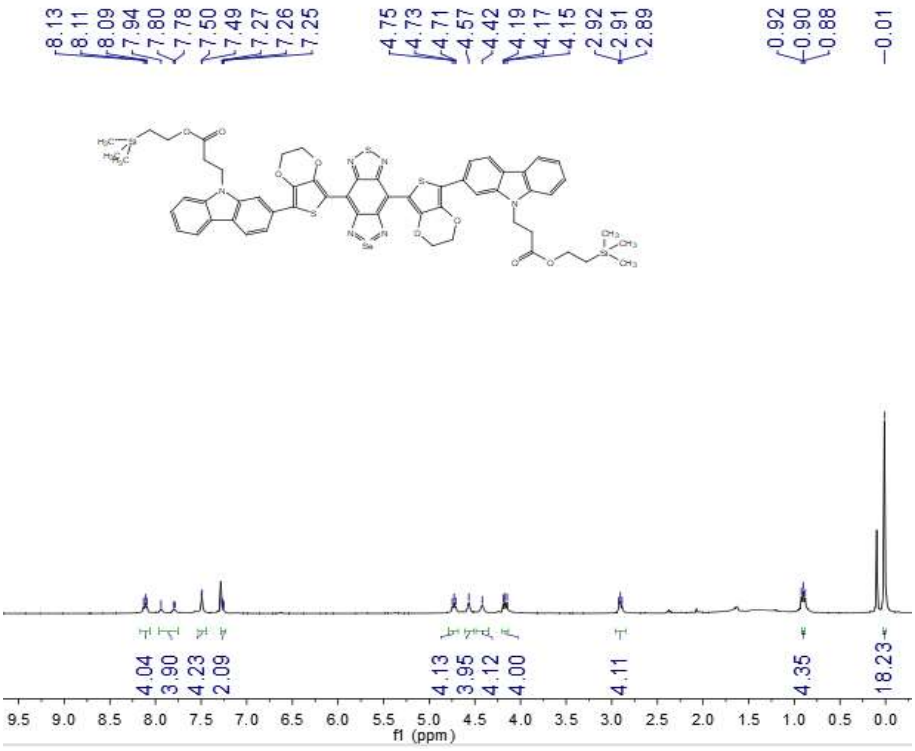

Figure S9. ^{1}H NMR spectrum (400 MHz, $CDCl_3$, 298 K) of **Se-IR1100**.

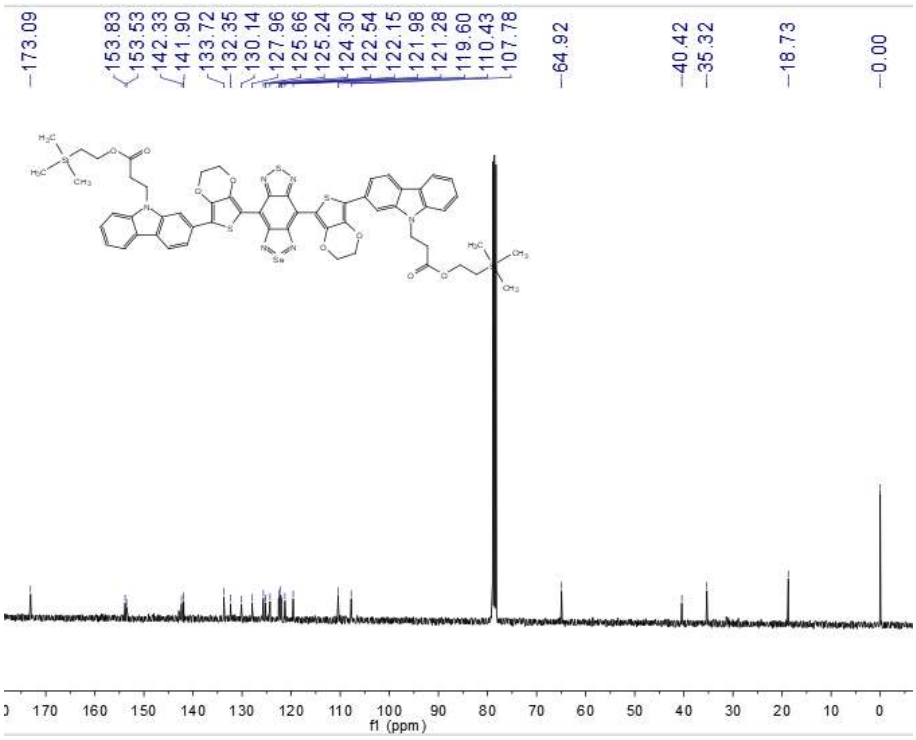

Figure S10. ^{13}C NMR spectrum (400 MHz, CDCl3, 298 K) of **Se-IR1100**.

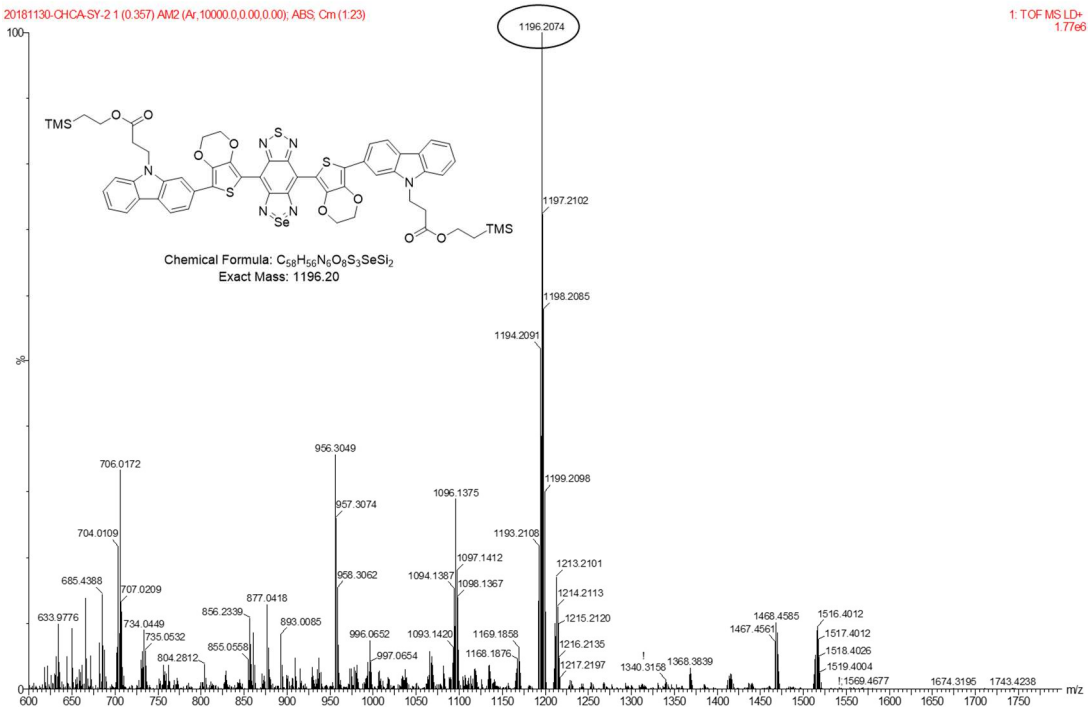

Figure S11. The MALDI-TOF-MS of **Se-IR1100**.

Supporting Figures:

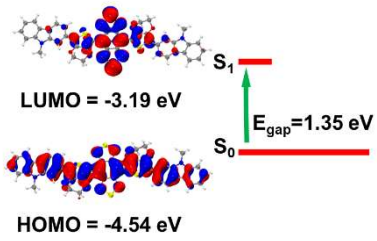

Figure S12. Calculated HOMO and LUMO with orbital energies [1.35 eV] for **Se-IR1100** NPs at the DFT B3LYP/6-31G basis set level of theory.

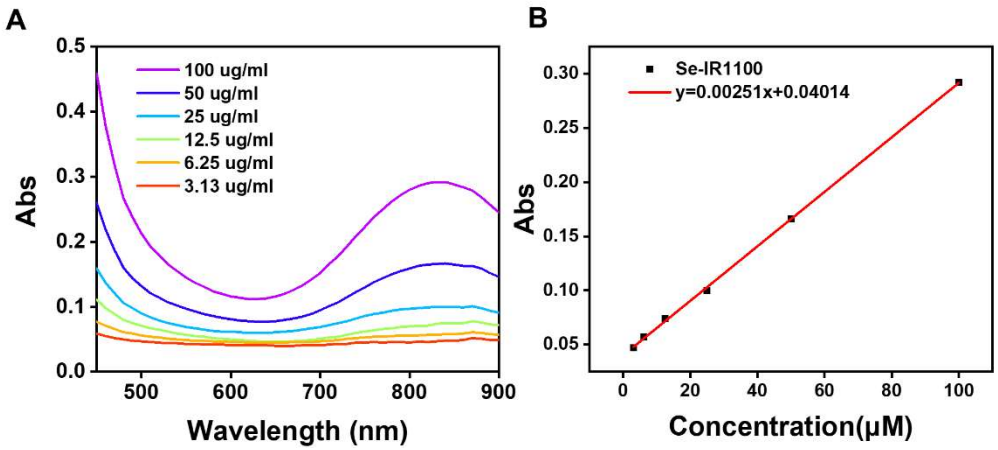

Figure S13. A) The relative absorbance of **Se-IR1100** of in the UV-vis spectrum at 845 nm. B) The calibration curve was linear in the range of 3.12 - 100 μg/ml with a correlation coefficient of $R^2 = 0.997$. The encapsulation efficiency was defined as the ratio between the amount of **Se-IR1100** encapsulated in the DSPE-mPEG5000. The organic dye **Se-IR1100** encapsulation efficiency of **Se-IR1100** NPs was 58.2 ± 1.4%.

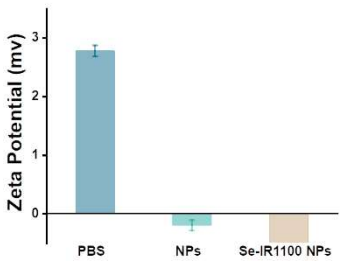

Figure S14. Zeta potential of PBS, NPs, and **Se-IR1100** NPs.

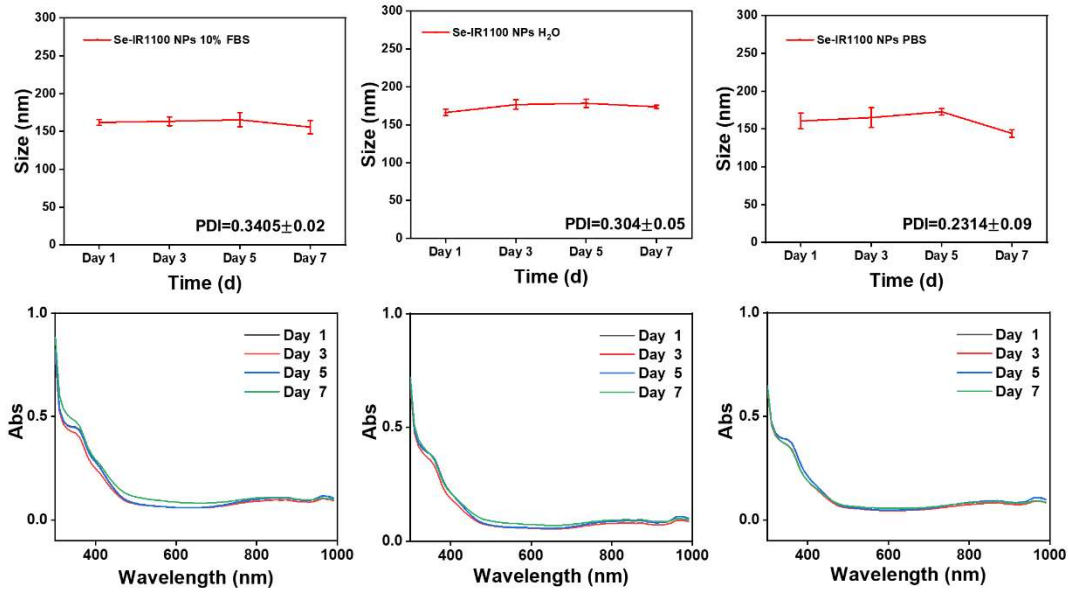

Figure S15. The DLS size of **Se-IR1100** NPs in 10% FBS, H_2O, and PBS and the stability of **Se-IR1100** NPs in 10% FBS, H_2O, and PBS for 7 days (the DLS and absorption in day 1, day 3, day 5, day 7).

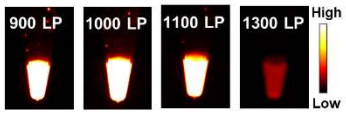

Figure S16. Fluorescence imaging images of **Se-IR1100** NPs in different filters (900 LP, 1000 LP, 1100 LP, 1300 LP) under 808 nm irradiation (200 ms, 30 mW cm^{-2}).

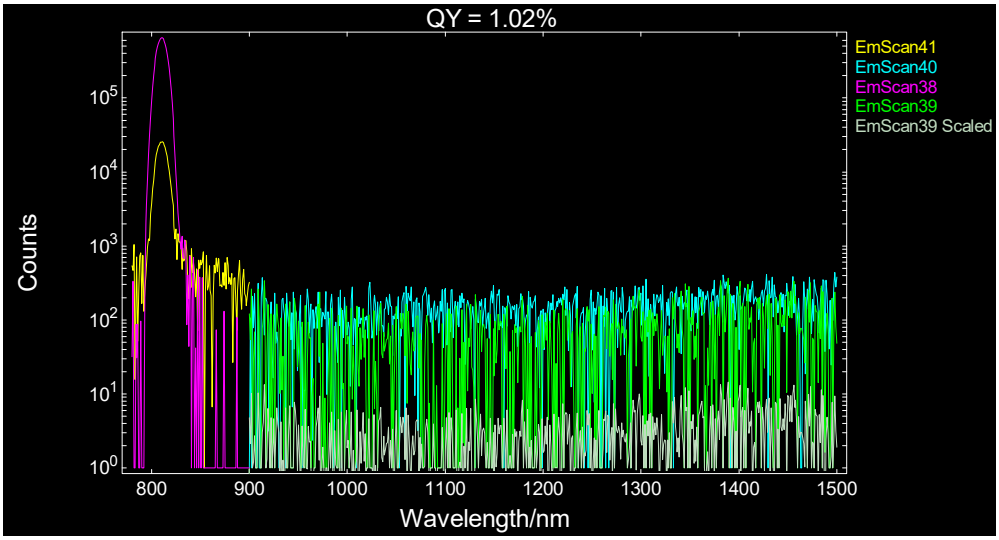

Figure S17. The absolute photoluminescence quantum yield (PLQY) of Se-IR1100 NPs.

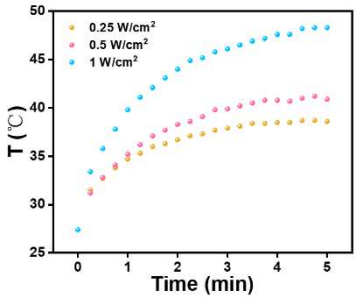

Figure S18. The temperature change of **Se-IR1100** NPs under different power irradiation of 808 nm laser.

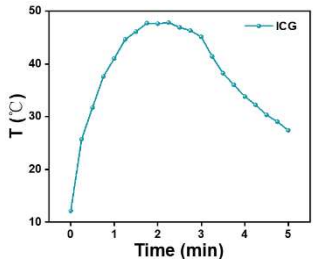

Figure S19. Temperature change of the ICG at 40 μM after 808 nm irradiation 5 min.

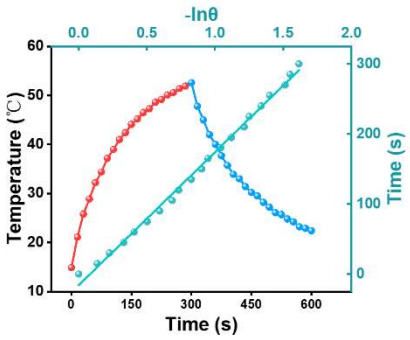

Figure S20. Monitored temperature profile (red line) of **Se-IR1100** NPs illuminated for 300 s and followed by natural cooling, and linear time data versus –lnθ (blue line) from the cooling period.

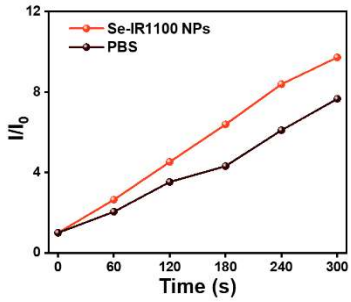

Figure S21. ROS generation of **Se-IR1100** NPs (20 μM) under 808 nm irradiation at different time.

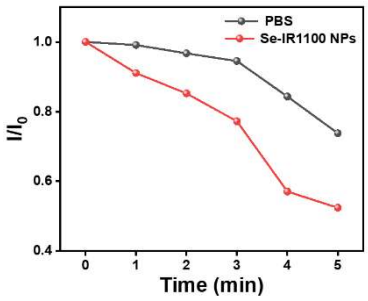

Figure S22. $^1O_2$ generation of **Se-IR1100** NPs (20 μM) under 808 nm irradiation at different time.

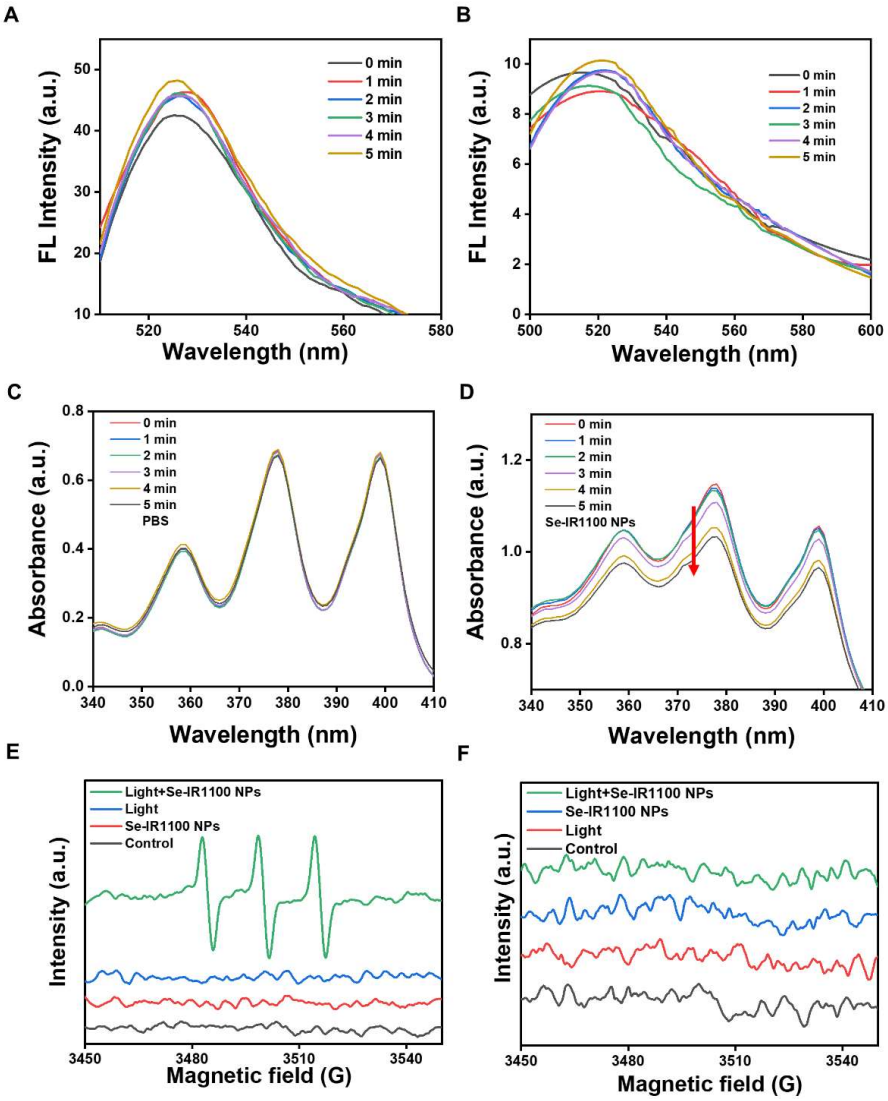

Figure S23. (A) HPF and (B) DHR123 were used as indicators to detect the Se-IR1100 NPs generation ·OH and $\cdot O_2^-$ under light conditions respectively. (C) $^1O_2$ generation of PBS and (D) **Se-IR1100** NPs (20 μM) under 808 nm irradiation at different time. (E) The TEMP and (F) DMPO were used as $^1O_2$ and ·OH trapping agents, respectively.

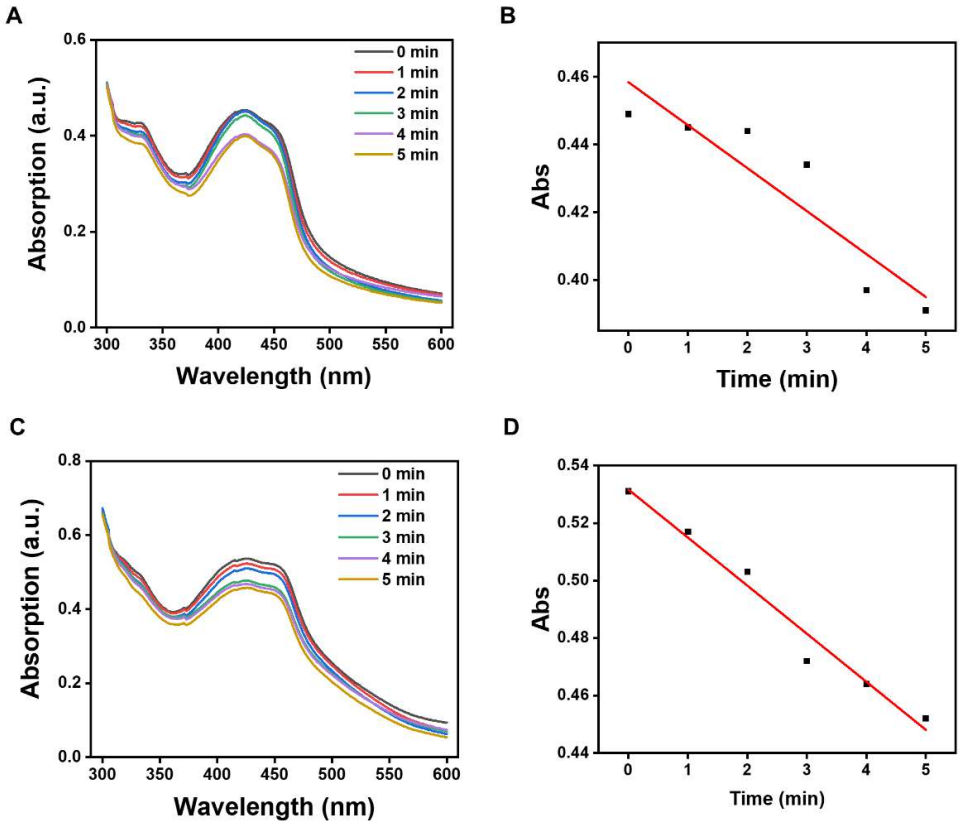

Figure S24. (A)$^1O_2$ generation of Se-IR 1100 NPs (20 μM) and ICG (20 μM) (C) using DPBF as a probe with 808 nm laser illumination (1 W cm^{-2}) for various time. Linear calibration curve for the absorbance of DPBF plus Se-IR 1100 NPs (B) or ICG (D) to illumination time.

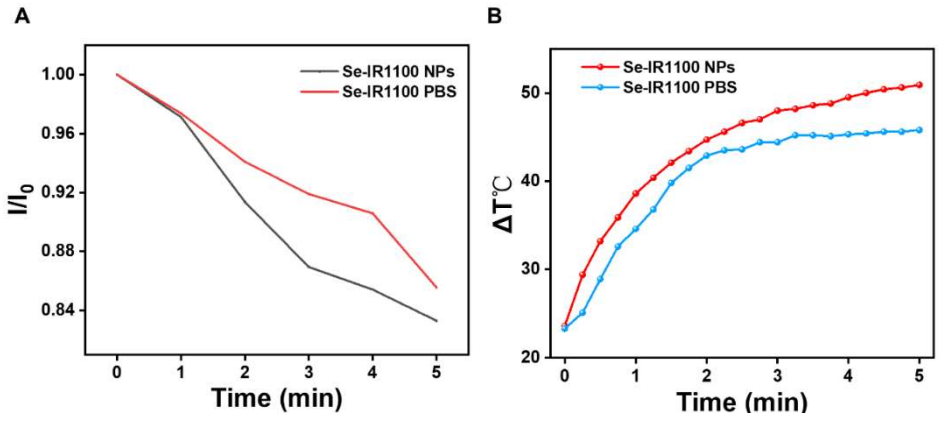

Figure S25. (A) $^1O_2$ generation of Se-IR1100 NPs (20 μM) and Se-IR1100 (20 μM) in PBS under 808 nm irradiation at different time with DPBF as an indicator. (B) Temperature change curves of the Se-IR1100 NPs (20 μM) and Se-IR1100 (20 μM) in PBS under 808 nm irradiation at different time.

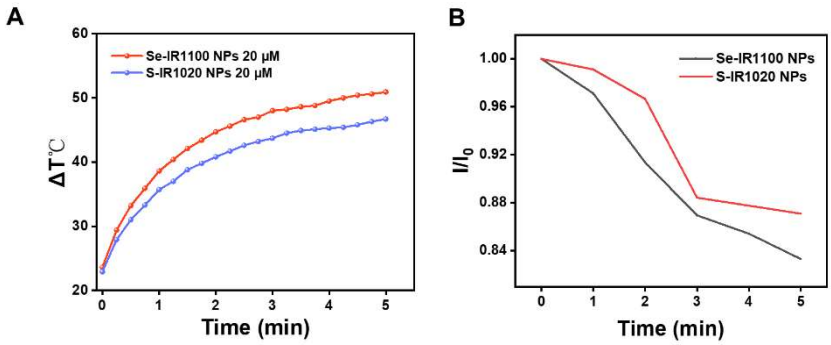

Figure S26. (A) Temperature change curves of the Se-IR1100 NPs (20 μM) and S-IR1020 NPs (20 μM) in PBS under 808 nm irradiation at different time. (B) $^1O_2$ generation of Se-IR1100 NPs (20 μM) and S-IR1020 NPs (20 μM) in PBS under 808 nm irradiation at different time with DPBF as an indicator. (S-IR1020 represents the D-A-D structure fluorophore replaced by S atom)

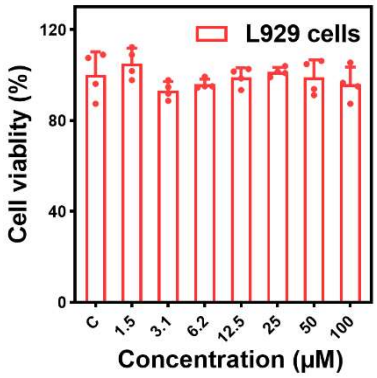

Figure S27. Cells viability incubated with **Se-IR1100** NPs at different concentrations.

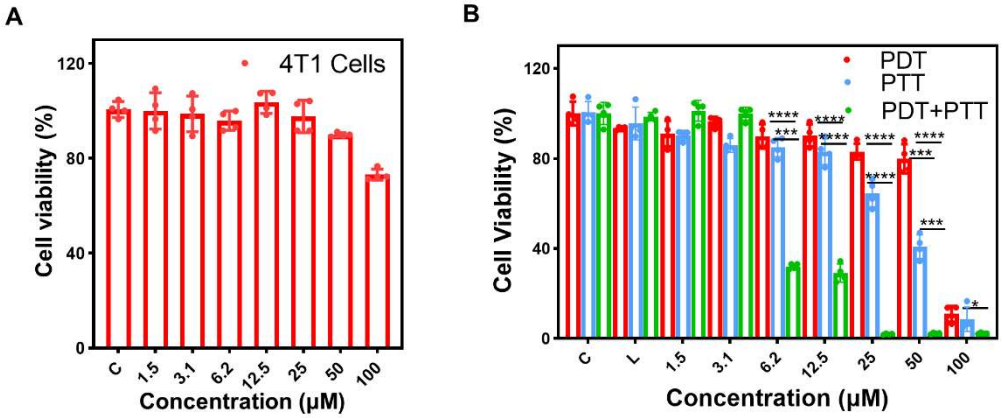

Figure S28. (A) 4T1 cells viability incubated with **Se-IR1100** NPs at different concentrations. (B) 4T1 cells viability of the PTT, PDT, and PDT + PTT therapy with **Se-IR1100** NPs at different concentrations with 808 nm laser irradiation (1.0 W cm^{-2}) for 5 min.

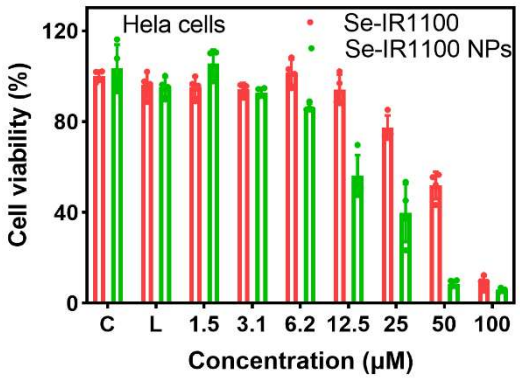

Figure S29. The cell viability of Hela cells after the PDT + PTT therapy with Se-IR1100 NPs and Se-IR1100 at different concentrations under 808 nm laser.

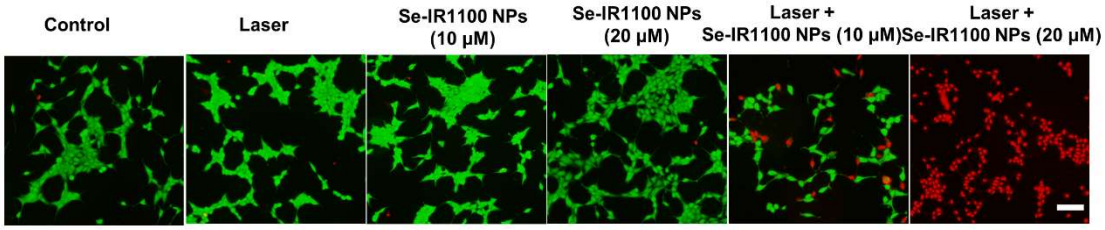

Figure S30. Live (calcein AM)/dead (PI) dual-staining of HeLa cells under different treatments. Scale bar: 30 μm.

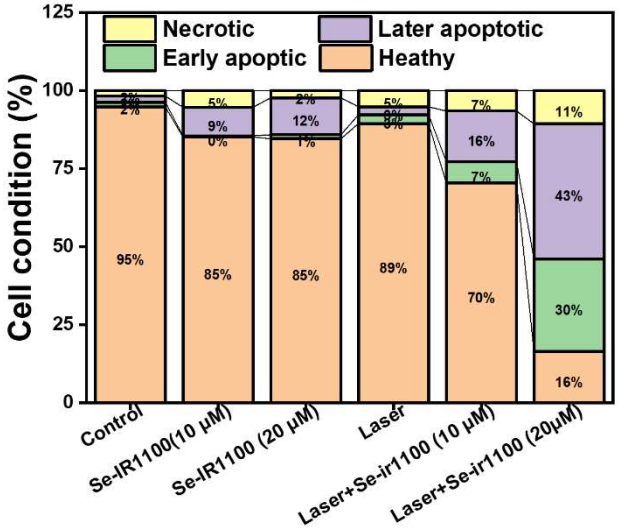

Figure S31. The apoptotic rate of HeLa cells with different treatment.

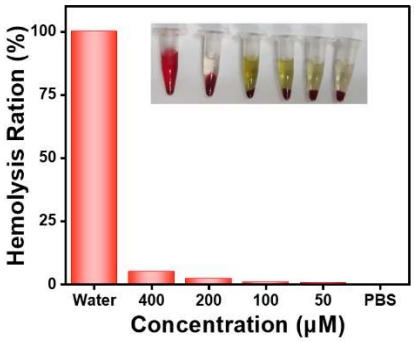

Figure S32. Effects on hemolysis rate of erythrocytes at different concentrations of **Se-IR1100** NPs (50 to 400 μM).

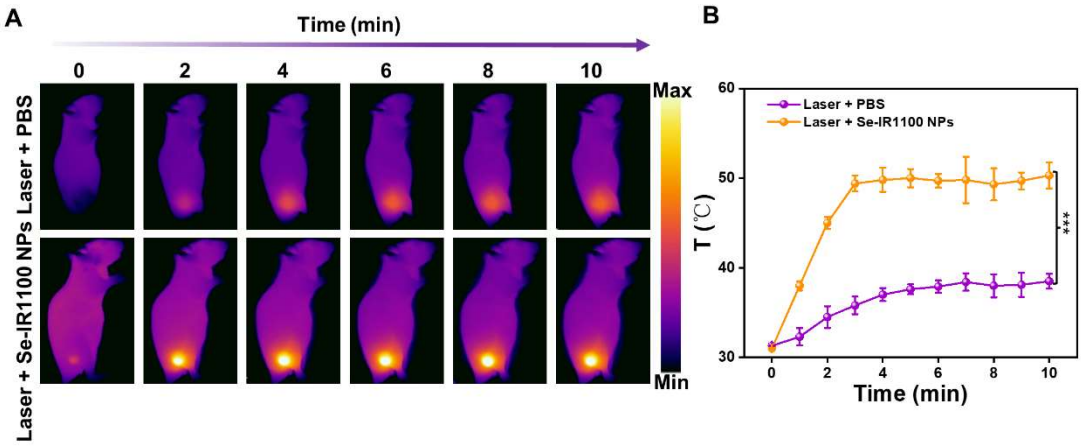

Figure S33. (A) Thermal images after intravenous injection of **Se-IR1100** NPs or PBS in treated with 808 nm laser *in vivo* (200 μM, 200 μL). (B) The temperature change curves of **Se-IR1100** NPs or PBS in treated with 808 nm laser *in vivo* from (A).

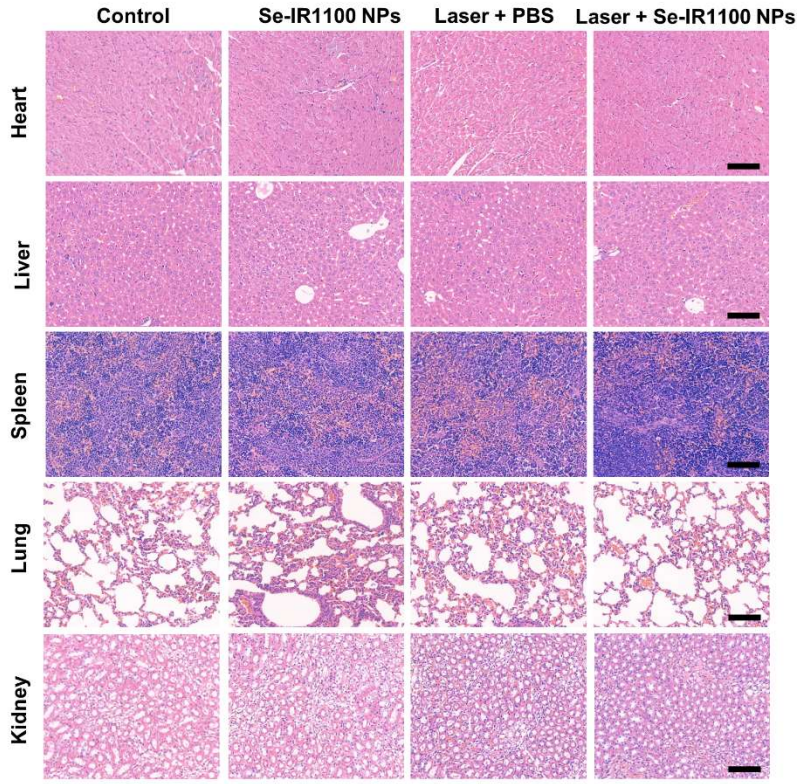

Figure S34. H&E staining images of main organs (heart, liver, spleen, lung and kidney) from different groups after treatments. Scale bar: 100 μm.

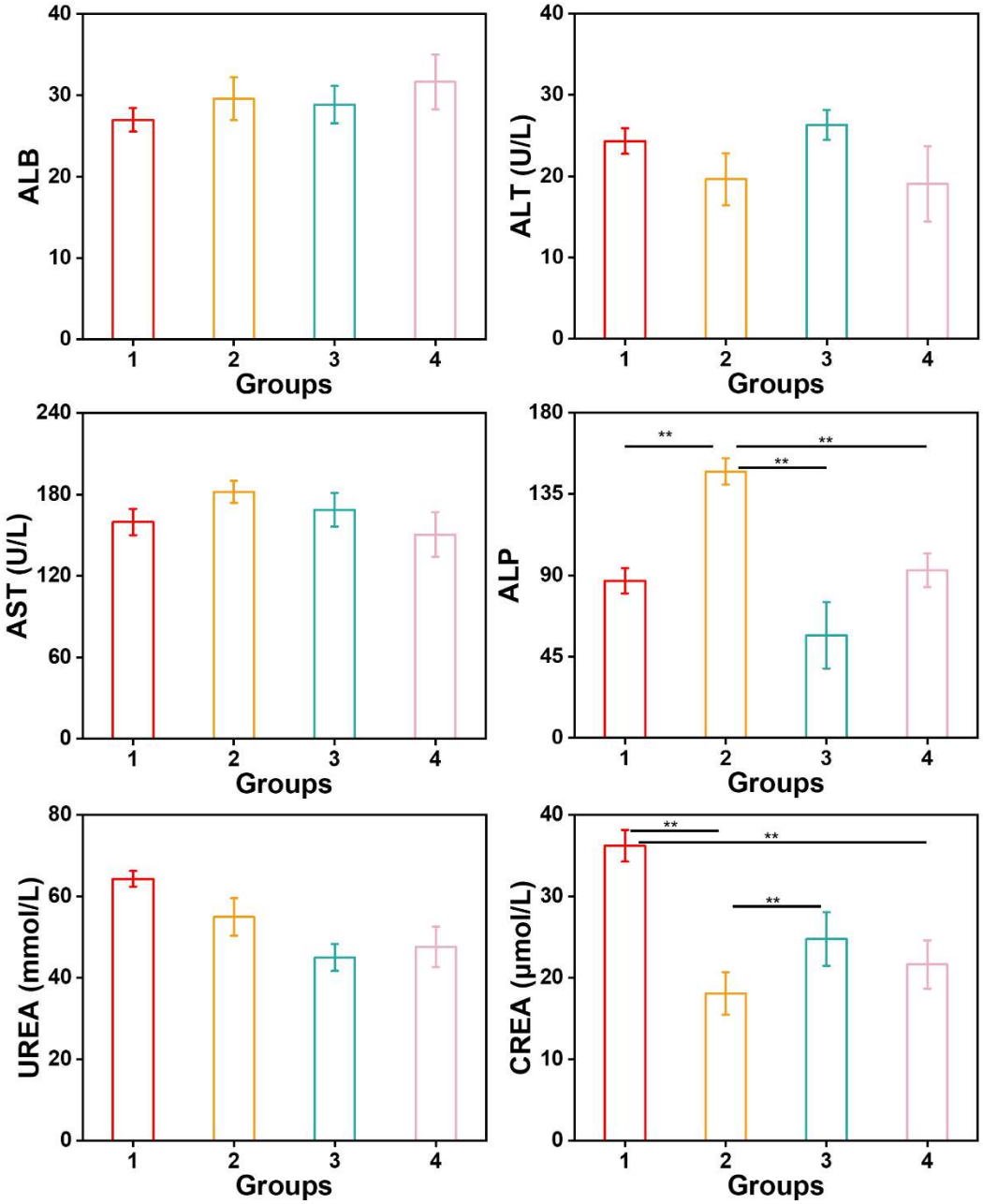

Figure S35. Safety assessment of **Se-IR1100** NPs in mice. Mice for evaluation of liver and kidney functions from different groups. n = 3. Abbreviations: AST, glutamic oxaloacetic transaminase (36.31 - 235.48); ALT, alanine aminotransferase (10.06 - 96.47); ALP, alkaline phosphatase (22.52 - 474.35); ALB, albumin (21.22 - 39.15); UREA, urea (30.27 - 97.27); CREA, creatinine (10.91 - 85.09).

References

1 W. Tao, X. Cheng, D. Sun, Y. Guo, N. Wang, J. Ruan, Y. Hu, M. Zhao, T. Zhao, H. Feng, L. Fan, C. Lu, Y. Ma, J. Duan and M. Zhao, *Biomater.*, 2022, **287,** 121621.

2 X. Zhang, C. Li, Y. Zhang, X. Guan, L. Mei, H. Feng, J. Li, L. Tu, G. Feng, G. Deng and Y. Sun, *Adv. Funct. Mater.*, 2022, **32,** 2207259.

3. T. Yang, L. Liu, Y. Deng, Z. Guo, G. Zhang, Z. Ge, H. Ke and H. Chen, *Adv. Mater.,* 2017, **29**, 1700487.